Commun Nonlinear Sci Numer Simulat 39 (2016) 233–247

Contents lists available at ScienceDirect

Commun Nonlinear Sci Numer Simulat

journal homepage: www.elsevier.com/locate/cnsns

Refined two-index entropy and multiscale analysis for complex system

Songhan Bian, Pengjian Shang*

Department of Mathematics, School of Science, Beijing Jiaotong University, Beijing 100044, PR China

ARTICLE INFO

Article history:
Received 5 April 2015
Revised 29 January 2016
Accepted 11 March 2016
Available online 19 March 2016

Keywords:
Complex system
Refined two-index entropy
Scaling exponent

ABSTRACT

As a fundamental concept in describing complex system, entropy measure has been proposed to various forms, like Boltzmann–Gibbs (BG) entropy, one-index entropy, two-index entropy, sample entropy, permutation entropy etc. This paper proposes a new two-index entropy $S_{q,\delta}$ and we find the new two-index entropy is applicable to measure the complexity of wide range of systems in the terms of randomness and fluctuation range. For more complex system, the value of two-index entropy is smaller and the correlation between parameter δ and entropy $S_{q,\delta}$ is weaker. By combining the refined two-index entropy $S_{q,\delta}$ with scaling exponent $h(\delta)$, this paper analyzes the complexities of simulation series and classifies several financial markets in various regions of the world effectively.

1. Introduction

In many modern sciences, like physics, economics, biology, quantum information theory, complex system etc., the concept of entropy is a fundamental concept. Many attempts have been done to propose new entropy measure forms in the past several decades. The Boltzmann–Gibbs (BG) statistical entropy,

$$S_{BG} = -k\sum_{i=1}^{W} p_i \ln p_i \tag{1}$$

where $\sum_{i=1}^{W} p_i = 1$, is one of the most successful theories, which provides a powerful algorithm to understand how fast the thermodynamics of a system on much larger space-time scales is affected by microscopic physics with short-range interactions [1,2]. The well-known Boltzmann–Gibbs statistical mechanics is based on the Boltzmann–Gibbs entropy. Also, by assuming the ergodic or chaotic hypothesis, Boltzmann–Gibbs statistical mechanics has been successfully adopted in the description of mechanical phenomena and in nonequilibrium statistical mechanics [2,3].

Boltzmann–Gibbs statistical mechanics can typically describe systems which are characterized by weak correlation and short-range interactions, however there are some complex and multifractal systems which exceed domain of applicability for Boltzmann–Gibbs entropy. For example, long-range-interaction Hamiltonian systems and nonlinear dynamical systems at the edge of chaos. It also turned out to be not enough for various complex natural, social, and artificial systems, such as when a zero maximal Lyapunov exponent is present [4]. In order to deal with these systems, several nonextensive statistical mechanics which emerged from the standard Boltzmann–Gibbs entropy were presented. One of the most important generalization

* Corresponding author. Tel.: +86 13641228092.
E-mail addresses: 11271029@bjtu.edu.cn (S. Bian), pjshang@bjtu.edu.cn (P. Shang).

http://dx.doi.org/10.1016/j.cnsns.2016.03.007
1007-5704/

of the BG theory [5–7] which was introduced by Tsallis in 1988, is characterized by index q. $S_q = k(1 - \sum_{i=1}^{W} p_i^q)/(q-1)$ and this form derived from the works of Cressie and Read in 1984 [8,9]. That entropy was successful in widening the range of applicability of statistical mechanical concepts to many complex systems. And since then, a considerable progress which contributes to various functions, distributions and important equations was achieved [7]. In recent years, with the development of thermodynamics, many optimization methods have been widely applied to some thermodynamic fields, especially heat flux. For instance, some optimal designs based on classic optimization methods, like entropy generation minimization (EGM) and genetic algorithm (GA), have been proposed to optimize Reynolds number for developed laminar forced convection, improve heat transfer for laminar forced convection and optimize architecture of heat generating pieces [10–22].

Some related concepts have been proposed, like *additive*, *extensive* and *nonextensive* [23,24]. For a system A, a quantity $Y(A)$ is known as *additive* with regard to a specific composition of $A_1, A_2, \ldots, A_N$ if it satisfies

$$Y\left(\sum_{i=1}^{N} A_i\right) = \sum_{i=1}^{N} Y(A_i) \tag{2}$$

where $+$ inside the argument of Y precisely indicates that composition. Another related concept is *extensivity*. $Y(A)$ is *extensive* if

$$\lim_{N\to\infty} \frac{|Y(N)|}{N} < \infty \tag{3}$$

with the notation $Y(N) \equiv Y(\sum_{i=1}^{N} A_i)$. Apparently, all quantities which are additive are also extensive. However, there are some quantities that are neither additive nor extensive and they are called *nonextensive*. Nonenxtensive statistical mechanics first introduced in 1988 is the entropy S_q mentioned above. By focusing on complex systems with surface-dominant statistics, Hanel and Thurner found nonadditive entropic forms can be used to re-establish the entropic extensivity of the system in 2011 [25]. The concept of extensivity has been investigated mostly for independent systems. Assuming that systems are statistically independent, for systems A and B, it follows that: $S_{BG}(A+B) = S_{BG}(A) + S_{BG}(B)$. Thus, BG entropy is additive and extensive, but for S_q, we have $S_q(A+B) = S_q(A) + S_q(B) + (1-q)S_q(A)S_q(B)$. Hence, S_q is nonextensive for $q \neq 1$. In Ref. [26], Tsallis has illustrated the outstanding changes when A and B are specially correlated. In such case, $S_{BG}(A+B) \neq S_{BG}(A) + S_{BG}(B)$ and $S_q(A+B) = S_q(A) + S_q(B)$. Therefore, BG entropy is not extensive in the case of correlated systems [27].

At the same time, a candidate of the black hole thermodynamic entropy has been emerged recently [28–30], namely, $S_\delta = k\sum_{i=1}^{W} p_i \ln^\delta \frac{1}{p_i}$ $(\delta > 0)$. The entropy has been studied recently, particularly its equilibrium distribution and associated nonlinear Fokker–Planck equation [31]. At the same time, some other entropy forms were suggested depending on one parameter [32–35]. A group of two parameters entropies was also presented in the Refs. [36–39]. In particular the black hole thermodynamical entropy [29], and the Hanel–Thurner entropy $S_{c,d}$ [25,40]. Komatsu and Kimura proposed one entropic-force model deriving from this black-hole entropy to examine entropic cosmology in 2013 [30]. Also, other entropies have been introduced which are described by three parameters [41]. In addition, there are some entropies with arbitrary concave function instead of logarithm known as the Rényi entropy and its generations [42–44].

In this work, we will start with maximizing the entropy measure and transforming the specific thermodynamic nonextensivity to extensivity. As it is known, a usual procedure to find the probability distribution of a system is maximizing the entropy measure under normalization and energy constraints [45]. Assuming the system is constituted by some basic elements, we will introduce a new two-index entropy $S_{q,\delta}$ by analyzing the maximization of entropy for the case of equal probabilities of elements. The elements of this system are generated from the basic elements via a specific model. The refined two-index entropy can been seen as a generalization of unifying the well-known one-parameter nonextensive entropy S_q and one-parameter entropy S_δ. In the latter part, we will carry out the multi-scaling analysis [46] on the two-index entropy measure of series. Multi-scale method is a significant perspective to investigate complex systems, thermodynamics and optimization process. The study of multi-scale flows has become a subject of keen interest to develop advanced configurations capable of rendering maximum heat transfer density. Also, multi-scale design based on constructal theory has been applied to estimate the optimal insulated spacing, heaters size and heat generation rates [47–50]. By simulation experiments we can obtain some reference data and then the application in real series will be taken. Several financial markets will be classified by multi-scale theory and the two-index entropy $S_{q,\delta}$.

The paper is organized as follows. In Section 2, a brief review of BG-entropy and two one-parameter entropies S_q and S_δ, will be presented. In Section 3, we will propose the two-index entropy $S_{q,\delta}$ by unifying the one-parameter entropies S_q and S_δ, and introduce the multi-scaling analysis of two-index entropy $S_{q,\delta}$. In Section 4, several simulation experiments will be taken to examine the performance of the two-index entropy $S_{q,\delta}$ and scaling exponent $h(\delta)$. In Section 5, the two-index entropy $S_{q,\delta}$ and scaling exponent $h(\delta)$ will be applied to analyze the financial markets and classify them. Finally, we will present conclusions in Section 6.

2. Boltzmann–Gibbs entropy and two one-parameter entropies

Nowadays, many complex systems cannot be described by BG statistical mechanics and generating the entropy forms from BG entropy turns to be necessary to recover thermodynamic extensivity for nonstandard systems. In social and

physical systems, complexity usually emerges because of long-term memory, multifractality, spatio-temporal long-range correlations between the elements and some other dynamical ingredients. The frame of extensive statistical mechanics has been generalized to various applications, including predictions, high-energy physics [51], self-organized criticality [52] and others. We will describe briefly two one-index entropy functional forms S_q and S_δ, which are generalizations of BG entropy. Many complex systems will also be introduced as below [7,28].

We know that if a complex system is constituted by N elements, which are independent, we can get the number of the probable processes:

$$W(N) \sim A\xi^N \quad (A > 0, \xi > 1) \tag{4}$$

Take coin tossing as an example and we have $W = 2^N$ for N independent coins. In the system where all the processes have equal probabilities, $p = \frac{1}{W}$, using BG entropy Eq. (1), we can immediately verify that

$$S_{BG}(N) = k_B \ln W(N) \sim k_B(\ln \xi)N \propto N \tag{5}$$

According to Eq. (2), the thermodynamic extensivity is satisfied for $W(N)$ in this case. Then we transform the system which generates the data or information. Considering the q-generalization of the central limit and Levy–Gnedenko theorems [53,54], strong correlations are present, assuming that

$$W(N) \sim BN^\tau (B > 0, \tau > 0) \tag{6}$$

In this case, using BG entropy Eq. (1), we have $S_{BG}(N) \propto \ln N$, which violates the thermodynamical extensivity (Eqs. (2) and (3)). S_q(see Eq. (7)), as a possibility for measuring complex systems, may be active. As a generalization of the BG theory, S_q currently is referred to as nonextensive statistical mechanics and it is also a nonadditive entropy.

$$S_q = k_B \sum_{i=1}^{W} p_i \left(\ln_q \frac{1}{p_i}\right) \tag{7}$$

where $\ln_q m = \frac{m^{1-q}-1}{1-q}$ and $\ln_1 m = \ln m$. For $q = 1 - \frac{1}{\tau}$, we can verify that

$$S_q(N) = k_B \ln_q W(N) = k_B \frac{B^{1-q}N^{\tau(1-q)} - 1}{1-q} \propto N \tag{8}$$

According to Eq. (2), the thermodynamic extensivity is satisfied for $W(N)$ in this case. For S_q, the case $q = 1$ recovers S_{BG}. Some probabilistic and physical models are respectively available which belong to this case in [55–57].

In fact for the other case where $W(N)$ is smaller than Eq. (4) and larger than Eq. (6), just as:

$$W(N) \sim C\beta^{N^\gamma} \quad (C < 0, \beta > 1, 0 < \gamma < 1) \tag{9}$$

when $\gamma \to 1$, the target entropy is S_{BG}. For $0 < \gamma < 1$, we easily know that S_q and S_{BG} do not succeed in recovering thermodynamic extensivity here. But, the appropriate entropy is already available in the literature [29], namely

$$S_\delta = k_B \sum_{i=1}^{W} p_i \ln^\delta \frac{1}{p_i} \quad (\delta > 0) \tag{10}$$

It is easily verified that, if $W(N)$ satisfies Eq. (9), for $\delta = \frac{1}{\gamma}$, it shows

$$S_\delta(N) = k_B \ln^\delta W(N) = k_B(\ln C + N^\gamma \ln \beta)^\delta \sim k(\ln \beta)N \propto N \tag{11}$$

According to Eq. (2), the thermodynamic extensivity is satisfied for $W(N)$ in this case. Obviously, the case $\delta = 1$ also recovers S_{BG}. As a function of the index δ and the probability p , entropy S_δ concaves for $0 < \delta \le (1 + \ln W)$.

From what we have mentioned above, S_{BG}, S_q and S_δ can address some specific complex systems. For the case of equal probabilities, they recover the thermodynamical extensivity successfully and they will constitute one of the contributions of this paper work.

3. Refined two-index entropy and multi-scale analysis

3.1. The refined two-index entropy

From Eqs. (6) and (8), if a system is constituted by N elements and $W(N) \sim BN^\tau$, we have $S_q(N) \propto N$ and $S_q(N)$ is extensive. We can draw the conclusion that the entropy $S_q(N)$ is extensive even if $W(N) \sim B(N)N^\tau (B > 0, \tau > 0, N \to \infty)$, $B(N)$ being any function satisfying $\lim_{N\to\infty} \frac{B(N)}{N^\tau} = 0$.

At the same time, for S_δ, indeed we can verify $S_\delta(A + B) \neq S_\delta(A) + S_\delta(B)$ for probabilistically independent systems A and B, however, $W^{A+B} = W^A W^B$ for the W satisfies Eq. (9). For equal probabilities, We have $S_\delta(N) = k \ln^\delta W(N)$. Hence, when $\delta > 0$,

$$\left(\frac{S_\delta(A+B)}{k}\right)^{\frac{1}{\delta}} = \left(\frac{S_\delta(A)}{k}\right)^{\frac{1}{\delta}} + \left(\frac{S_\delta(B)}{k}\right)^{\frac{1}{\delta}}. \tag{12}$$

In Section 2, we have known for $\delta = \frac{1}{\gamma}$, $S_\delta(N)$ is extensive. Considering Eq. (12), for the case of equal probabilities and $\delta > 0$, the form of $(S_\delta(N))^{\frac{1}{\delta}}$ make the thermodynamic extensivity satisfied for probabilistically independent systems.

Thus based on one-index entropy S_q, we unify these two one-index entropy forms (S_q and S_δ) as follow, which we call the refined two-index entropy:

$$S_{q,\delta} = k\left(\sum_{i=1}^{W} p_i(\ln_q \frac{1}{p_i})^\delta\right)^{\frac{1}{\delta}} \quad (q \in R, \delta > 0) \tag{13}$$

where $\ln_q m = \frac{m^{1-q}-1}{1-q}$ and $\ln_1 m = \ln m$.

It is obvious that S_q and S_δ are the particular cases for the two-index entropy $S_{q,\delta}$ just as $S_{q,1}$ and $S_{1,\delta}$, respectively, $S_{1,1} = S_{BG}$. As everyone knows, for equal probabilities $p = \frac{1}{W}$, the complexity of the series turns to be biggest and the value of entropy measure is also biggest. In this case we have

$$S_{q,\delta}(N) = k\ln_q W(N) \tag{14}$$

which is same to the biggest entropy for S_q. Thus $S_{q,\delta}(N)$ is extensive for $p = \frac{1}{W}$. Eq. (14) has nothing with parameter δ, so for the case of equal probabilities, the change of parameter δ will have no impact on the value of entropy. Therefore, apart from the refined two-index entropy measure itself, the influence power of parameter δ can be used to measure the dispersion and complexity of a series. That is because the two-index entropy $S_{q,\delta}$ highlights the impact of the point which has bigger dispersion in a series.

In the case of $q \neq 1$, Eq. (13) turns to be:

$$\begin{aligned} S_{q,\delta} &= k_1\left(\sum_{i=1}^{W} p_i(\ln_q \frac{1}{p_i})^\delta\right)^{\frac{1}{\delta}} \\ &= k_1\left(\sum_{i=1}^{W} p_i \frac{((\frac{1}{p_i})^{1-q}-1)^\delta}{(1-q)^\delta}\right)^{\frac{1}{\delta}} \\ &= k_2 \frac{(\sum_{i=1}^{W} p_i(1-p_i^{q-1})^\delta)^{\frac{1}{\delta}}}{q-1} \end{aligned} \tag{15}$$

In the last step, we alter constant k_1 to k_2 in order to keep $S_{q,\delta}$ positive. The features of the two-index entropy versus the two parameters can be discovered from Eq. (15). We find if q is big enough, $(1-p_i^{q-1}) \to 1$, the parameter δ and probability p_i have a slighter impact on entropy. So, when $q \to 1$, parameter δ works actively. Actually, no matter the size of the probabilities, parameter q always makes $(1-p_i^{q-1})$ smaller for the case $q \to 1$ and then balance the influence of probability on entropy. On the other hand, for $0 < \delta < 1$, the part $(1-p_i^{q-1})^\delta$ in the numerator becomes closer to 1 than $(1-p_i^{q-1})$ and thus weakens the effect of parameter q on entropy. On the contrary, for $\delta > 1$, $(1-p_i^{q-1})^\delta$ will strengthen the effect of parameter q and probability p_i on the refined two-index entropy. It can be verified, Eq. (15) is a monotone increasing function versus parameter δ and a monotone decreasing function versus parameter q.

On the other hand, how does the probability p_i affect the entropy? We have known if a series is generated randomly, it has bigger value of entropy. In other word, that is similar with the case for equal probabilities $p = \frac{1}{W}$ and Eq. (13) turns to be

$$S_{q,\delta} = k\ln_q \frac{1}{p} \tag{16}$$

We have known that the value of entropy $S_{q,\delta}$ has nothing with parameter δ in this case above. For a series which is similar with the random sequence, the parameter δ has minimal effect on the value of entropy. In this case the entropy is the biggest. On the contrary, for a series generated by some specific periodic systems, the data will show some regular and the probabilities are not equal. In this case, there are some big probabilities and some small probabilities and the entropy is small. Actually, as what we said, no matter the size of the probabilities, parameter q always makes $(1-p_i^{q-1})$ smaller for $q \to 1$ and then balance the influence of probability on entropy. Using the two-index entropy, we can estimate the complexity of series by the value of two-index entropy directly. But for some case, the values of entropy measure are nearby, so it is hard to compare the complexities of them by the entropy measure directly. As what we have mentioned above, the influence which parameter δ has on the refined two-index entropy $S_{q,\delta}$ can also reflect the complexity of system. In order to measure the influence, we can take the scaling exponent $h(\delta)$ as an efficient method. In what follows, considering the particularity of parameter δ, the multi-scale theory will be used to analyze the new two-index entropy.

3.2. Multi-scale analysis

In fact, the complexity of a time series is not only shown as the value of entropy. The scaling properties can also describe the complexity. Suppose that the series x_k has known and we can calculate the probabilities p_i. And then we can obtain the

two-index entropy measure and draw the charts of $S_{q,\delta}$ versus q and δ. To determine the scaling behavior of the two-index entropy $S_{q,\delta}$, we will analyze log–log plots of $S_{q,\delta}$ versus q for each value of δ [47]. Several examples of this procedure will be shown in next section. If $S_{q,\delta}$ increases as a power-law: $S_{q,\delta} \sim q^{h(\delta)}$:

$$\left(\sum_{i=1}^{W} p_i \left(\ln_q \frac{1}{p_i}\right)^{\delta}\right)^{\frac{1}{\delta}} \sim q^{h(\delta)} \tag{17}$$

Then we can obtain the scaling exponent $h(\delta) \sim \frac{\ln S_{q,\delta}}{\ln q}$ by evaluating the logarithm of $S_{q,\delta}$ and q. At the same time, if Eq. (17) has been set up, it is obvious that

$$\sum_{i=1}^{W} p_i \left(\ln_q \frac{1}{p_i}\right)^{\delta} \sim q^{\delta h(\delta)} \tag{18}$$

By uniting Eqs. (15) and (17), we have the new scaling exponent function:

$$\frac{(\sum_{i=1}^{W} p_i (1 - p_i^{q-1})^{\delta})^{\frac{1}{\delta}}}{q-1} \sim q^{h(\delta)} \tag{19}$$

It is not easy to obtain the scaling exponent $h(\delta)$ directly from Eq. (17). However, getting inspired by MF-DFA [47], we can calculate the estimated value of $h(\delta)$ by logging the both sides and calculating the slope of fitting straight. Actually, the value of scaling exponent $h(\delta)$ has a direct correlation with entropy measure. It shows that bigger entropy means smaller $h(\delta)$ and bigger slope of fitting lines for $h(\delta)$. Thus scaling exponent $h(\delta)$ is an another effective index to measure entropy of series even the series is complex and similar with each other. We can explain it from another perspective. On the one hand, the value of two-index entropy can indicate the complexity of a series. Bigger value means more complex series. On the other hand, the influence that parameter δ has on the entropy $S_{q,\delta}$ is able to mirror the complexity. Less influence means more complex series. In order to measure the influence, we proposed the scaling exponent $h(\delta)$.

Obviously, for equal probabilities $p = \frac{1}{W}$, using Eq. (17), we can verify

$$\frac{W^{1-q} - 1}{1-q} \sim q^{h(\delta)} \tag{20}$$

$h(\delta)$ is a constant for a fixed q and the monofractal is shown. In this case, $h(\delta)$ is only determined by the system $W(N)$ which generates the series. For $p \neq \frac{1}{W}$, $h(\delta)$ are determined by parameter δ and then we can verify the series is multifractal versus parameter δ. Thus, we can see the slope of $h(\delta)$ versus δ can describe the fractal feature and complexity. As what we have find above, sometimes even if the slopes are approximate and the fractal features are similar, the different values of scaling exponent still distinguish the systems which generate the similar series.

In fact, a hierarchy of exponents similar to $h(\delta)$ has been introduced [58]. Eq. (18) is identical to Eq. (17) and we can obtain analytically the relation between the two sets of multi-fractal exponents $\tau(\delta) = \delta h(\delta)$. Thus we have shown that $h(\delta)$ is directly related to the classical multi-fractal scaling exponents $\tau(\delta)$.

Algorithm

In order to put the two-index entropy into use, the method we proposed above can be divided into five steps. Let us assume that observations are available as the original time series: $X = \{x_0, x_1, x_2, \ldots, x_n\}$.

Step A: Symbolize the time series and get the probability series $P = \{p_0, p_1, p_2, \ldots, p_n\}$. Dynamical aspects of time series may be analyzed by symbolizing dynamics. Here are several approaches of symbolic sequence construction, for example σ-method, Max–min-method and Binary Δ-coding-method [59]. We can also obtain the probability series $P = \{p_0, p_1, p_2, \ldots, p_n\}$ by partial method of Sample entropy [60] and Permutation entropy [61]. Certainly, method selection depends on the characteristics of the data.

Step B: Calculate the entropy measure $S_{q,\delta}$ for parameter variables q and δ. Set a applicable test range for parameters (q, δ) and the entropy measure can be obtained by probability series $P = \{p_0, p_1, p_2, \ldots, p_n\}$ and Eq. (13).

Step C: Compare and analyze the entropy measure $S_{q,\delta}$. Using three-dimensional images for entropy measure $S_{q,\delta}$ versus parameters (q, δ), or two-dimensional images for $S_{q,\delta}$ versus q and $S_{q,\delta}$ versus δ, we are able to compare the entropy measure, and analyze the discrete and trends of these curves. With this, the complexity of original time series has been estimated roughly.

Step D: Obtain the scaling exponent $h(\delta)$. Considering Eq. (17), we evaluate the logarithm on the two sides of Eq. (17). For fixed δ_i, the exponent $h(\delta_i)$ can be obtained based on fitting function.

Step E: Analyze the complexity of series and classify the complexity of real time series from several financial markets. In this part, the scaling exponent of real series will be compared with reference scaling exponent which we get them by specific simulation time series, and then the original time series can be located into some simulation series which have approximately similar scaling exponent $h(\delta)$. Finally, the complexity and regularity can be classified.

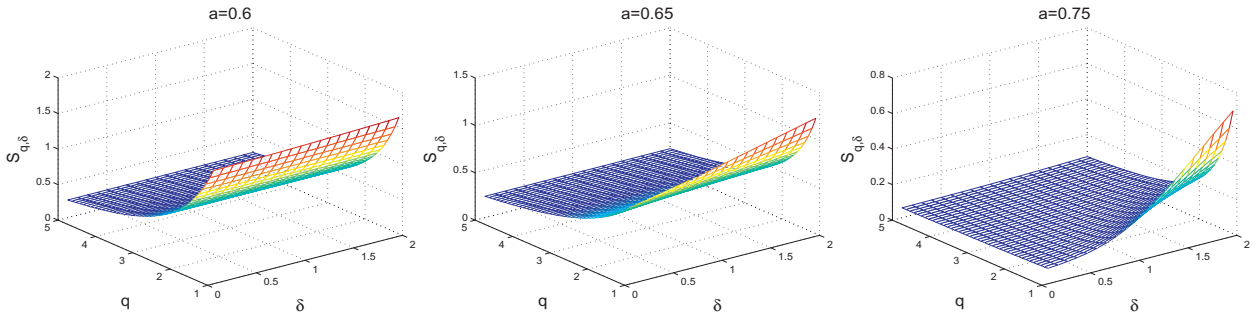

Fig. 1. The three-dimensional relationship between $S_{q,\delta}$, q and δ for the cases $a = 0.6$, $a = 0.65$ and $a = 0.75$.

4. Simulation examples

In this section, we will present several special test series to evaluate the effectiveness of the two-index entropy. To get a feeling for our entropy, we process not only the discrete chaotic maps, but orbits of several parametric families of dynamical systems. We set the sample size to be 6000 and the number of symbolic hierarchy to 20.

Proper range for q and δ**.** For the two-index entropy, We have known $\delta > 0$, thus we set the range is $0 < \delta \leq 2$ to measure the change of $S_{q,\delta}$ with the increasing of δ. It is obvious that $S_{q,\delta}(q)$ is continuous versus q, and for $0 < q \leq 1$, the property is same with the situation of $q > 1$. Thus in this paper, the case of $1 < q \leq 5$ will be studied as a testing example.

4.1. Binomial multifractal series

As the first example we apply the two-index entropy to binomial multifractal series. In the binomial multifractal model [58,62,63], a series of $N = 2^{max(n)}$ numbers k with $k = 1, \ldots, N$ is defined by

$$x_k = a^{n(k-1)}(1-a)^{max(n)-n(k-1)} \tag{21}$$

where $0.5 < a < 1$ is a parameter and $n(k)$ is the number of digits equal to 1 in the binary representation of the index k, e.g. $n(12) = 2$, since 12 corresponds to binary 1100.

There are different complexities for the sequences which are generated by different values of coefficient a. When a is small, the chaos is more obvious and the series is more complex. It also means regularity and forecasting feasibility is weak. On the contrary, for bigger a, the sequence shows some periodicity and the regularity and forecasting feasibility become more notable. So we just need to know whether the two-index entropy $S_{q,\delta}$ can show some obvious different features for different values of a. First, we survey the entropy function versus the two parameters. We picture them into a three-dimensional system of coordinate.

The graphs show that for different values of a which mean the complexities of the series are variant, the values of entropy function have different variation trends versus the two parameters. For $a = 0.6$, $a = 0.65$ and $a = 0.75$, we set as examples, and the entropies for $(q, \delta) = (1.1, 1)$ respectively are 1.6, 1 and 0.22. The gaps of entropy measure between the different series are obvious. It shows that the series when $a = 0.6$ is most complex and the case for $a = 0.75$ opposites by comparing the values of entropy measure directly.

To analyze the properties of the entropy function with two parameters, showing the families of curves is necessary. First of all, we study the characters of entropy $S_{q,\delta}$ versus δ. For each values of q from 1 to 5 and the step size is 0.1, we graph the relation between $S_{q,\delta}$ and δ. Then the families of curves are generated.

For $a = 0.6$, all the curves approximate parallel lines, because the value of δ affects the value of entropy infinitesimally for the high complexity of data. But when a becomes bigger and bigger, the impact of parameter δ turns to significant, shown as the latter two graphs in Fig. 1. In brief, stronger parallelism of the family of curves means more randomness and vice versa. Now, let us study the features of curves from another perspective. For each values of δ from 0 to 2 and the step size is 0.1, we graph the relation between $S_{q,\delta}$ and q. Then the families of curves are generated.

We can see that when $a = 0.6$, with the increasing of q from 1 to 5, for different parameter δ, the curves of $S_{q,\delta}$ versus q are very similar. It also means that if we fix the value of parameter q, the change of parameter δ has infinitesimal impact on $S_{q,\delta}$. When $a = 0.75$, with the increasing of q from 1 to 5, for different parameter δ, the gaps between disparate curves are outstanding. In brief, the close-knit family of curves reflects more randomness and dispersive family of curves shows more regular.

From what we have discussed above, the graphs shown as Figs. 2 and 3 can show the complexity of time series effectively. Thus the two-index entropy we proposed can describe the complexity and randomness of the time series by measuring the dispersion degree of the family of curves for $S_{q,\delta}$ versus q or parallelism degree of the family of curves for $S_{q,\delta}$ versus δ. Meanwhile, each line of the curves in Fig. 3 shows as a power-law approximatively. Thus we take $S_{q,\delta}$ and q in logs.

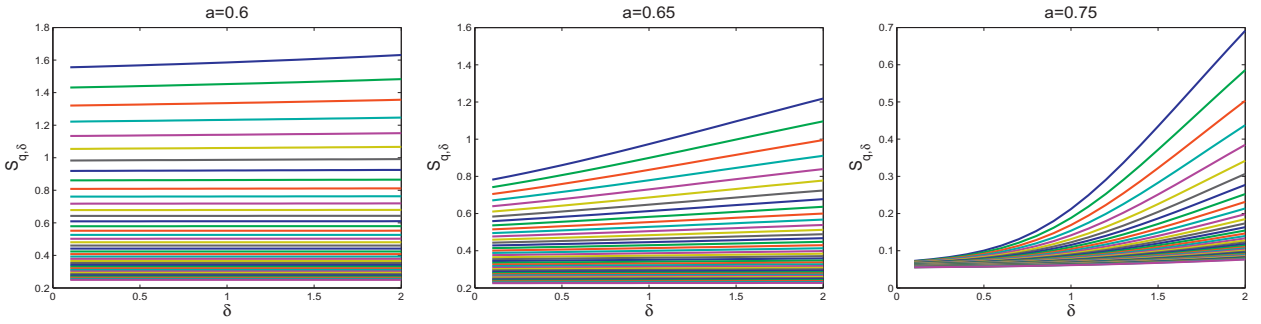

Fig. 2. Values of two-index entropy $S_{q,\delta}$ versus δ for the cases $a = 0.6$, $a = 0.65$ and $a = 0.75$. Curves of different colors represent different parameters q.

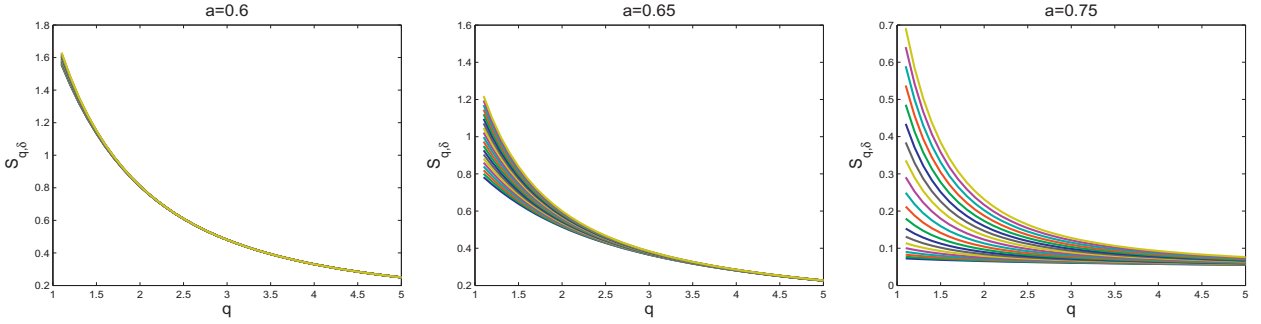

Fig. 3. Values of two-index entropy $S_{q,\delta}$ versus q for the cases $a = 0.6$, $a = 0.65$ and $a = 0.75$. Curves of different colors represent different parameters δ.

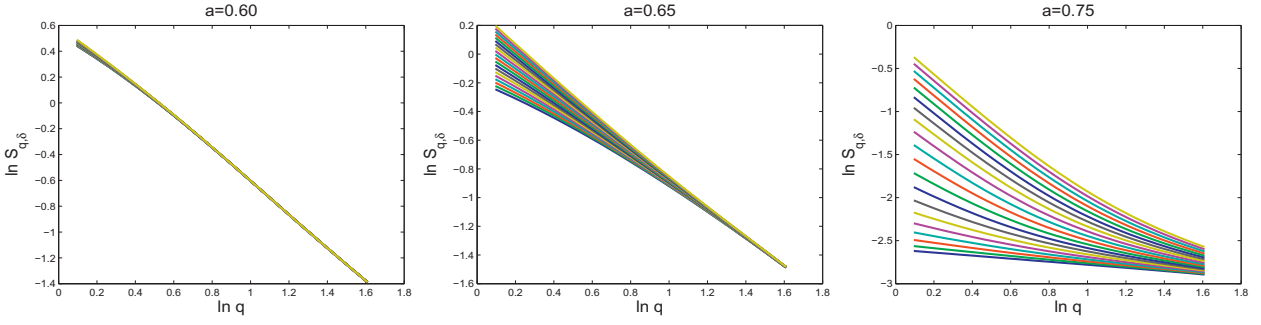

Fig. 4. Values of $\ln S_{q,\delta}$ versus $\ln q$ for the cases $a = 0.6$, $a = 0.65$ and $a = 0.75$. Curves of different colors represent different parameters δ.

From the chart above, $\ln S_{q,\delta}$ is approximately linear with $\ln q$. The slopes of these curves for different values of q are approximately equal and the power-law can be researched. Now we take statistical moments to measure the scaling behavior of binomial multifractal series based on the two-index entropy (see Figs. 4 and 5).

This graph tells us the two-index entropy detects the multifractal scaling exponents. For more complex sequence, δ has smaller effect on the scaling exponent $h(\delta)$. When $a = 0.6$, the two-index entropy shows monofractal approximatively, and for bigger a (for instance $a = 0.75$), it shows multifractal and scaling exponent $h(\delta)$ is determined by parameter δ. What we should stress is that for the two curves ($a = 0.6$ and $a = 0.65$), the slopes of scaling exponent versus δ is approximatively equal, but the values of scaling exponent are different. That is because the randomness of them is similar but the original systems $W(N)$ generating complexity are definitely different according to Eq. (20). In brief, the slope of the curves($h(\delta)$ versus δ) may reflect the randomness and the value of $h(\delta)$ can distinguish the source systems which affect the fluctuation range.

4.2. Gaussian White Noise

Gaussian White Noise is a series of uncorrelated (random) values, with Gaussian distribution. The probability density function is $f(x) = \frac{1}{\sqrt{2\pi}} exp(-\frac{x^2}{2})$. Using the algorithm we mentioned above, the entropy can be noted.

The first graph in Fig. 6 shows that the entropy $S_{q,\delta}$ increases with q approaching 1. And the different values of δ have a very minimal impact on the values of two-index entropy. The entropy measure is about 2.1 when $(q, \delta) = (1.1, 1)$.

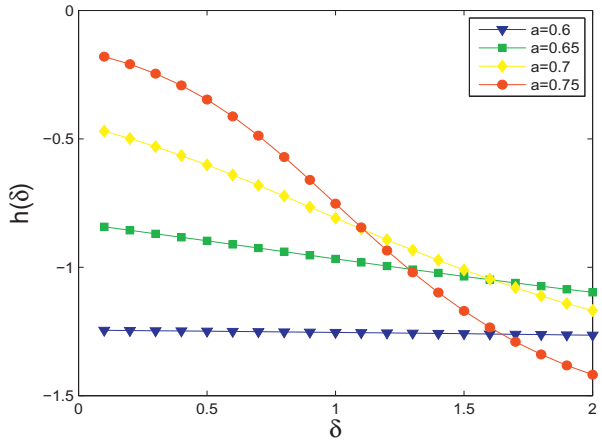

Fig. 5. The corresponding slopes $h(\delta)$ for four values of a together with results obtained from the best fitting straight lines of $\ln S_{q,\delta}$ versus $\ln q$ for each δ.

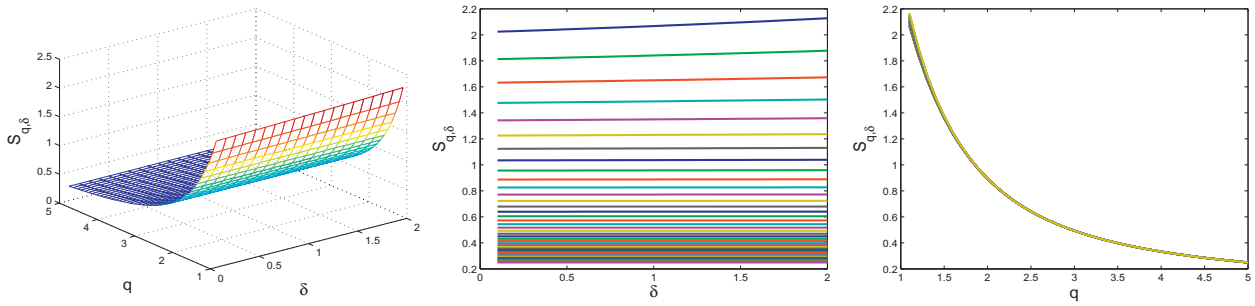

Fig. 6. The three-dimensional relationship between $S_{q,\delta}$, q and δ is shown in the first graph. The latter two graphs show the two-index entropy $S_{q,\delta}$ versus q and δ separately. Curves of different colors represent different parameters q for the second graph; curves of different colors represent different parameters δ for the third graph.

For Gaussian White Noise, based on the traditional fractal theory, the complexity degree is high in small scale. With the increasing of scale, the complexity of Gaussian White Noise decreases. The latter two graphs in Fig. 6 point the features of the first one from the other perspective. Because the sequence is generated randomly and is known as Gaussian White Noise, the probabilities turn to be approximately equal. Using Eq. (14), we can see that parameter δ has nothing to do with entropy $S_{q,\delta}$ approximately. Thus, the curves for different q are almost parallel in the second graph of Fig. 6 and the curves coincide with each other in the third graph of Fig. 6.

The curve in Fig. 7 can been seem as a horizontal straight line. By calculating the slope of the line, we can see the slope is approximatively equal to zero. It means for different scales, the complexities of Gaussian White Noise are similar based on the two-index entropy and the multi-scale theory.

4.3. Logistic map

As we know, the logistic map is often cited as an archetypal example of how complex, chaotic behavior can arise from very simple non-liner dynamical equations. The logistic map is a polynomial mapping of degree 2 and is often written as: $x_{n+1} = rx_n(1 - x_n)$. Where $0 < x_n < 1$ and the different values of the parameter r contribute to different behavior of the series. When r is small, the sequence is stable and the stability is independent of the initial value x_0; when $3 < r < 3.44...$, the sequence approaches to two different values. Then with the increasing of r, the periodic bifurcation becomes more and more. When the value of r increases to about 3.57, the periodic bifurcation is abrupt and chaos takes the place of periodicity. This paper takes $r = 2.9, r = 3.3, r = 3.7$ as examples.

In this case ($r = 2.9$, Fig. 8), because the sequence is stable and the stability is independent of the initial value, the complexity is small and the values of probabilities vary greatly. Fig. 8 shows that the curves of $S_{q,\delta}$ versus δ for different parameters q are not parallel and entropy $S_{q,\delta}$ has involvement with parameter δ apparently. $S_{q,\delta}$ is a monotone increasing function versus parameter δ and a monotone decreasing function versus parameter q. When parameter q is small, the entropy $S_{q,\delta}$ with different parameter δ vary greatly. The two-index entropy for the point $(q, \delta) = (1.1, 1)$ is about 0.24.

In this case ($r = 3.3$, Fig. 9), the original sequence approaches to two different values. The probabilities of the symbols also approach to two different values. Therefore, the impact of parameter δ recedes and curves of $S_{q,\delta}$ versus δ trend to be parallel. Also, the curves of $S_{q,\delta}$ versus q trend to assemble. The two-index entropy for $(q, \delta) = (1.1, 1)$ is about 0.7.

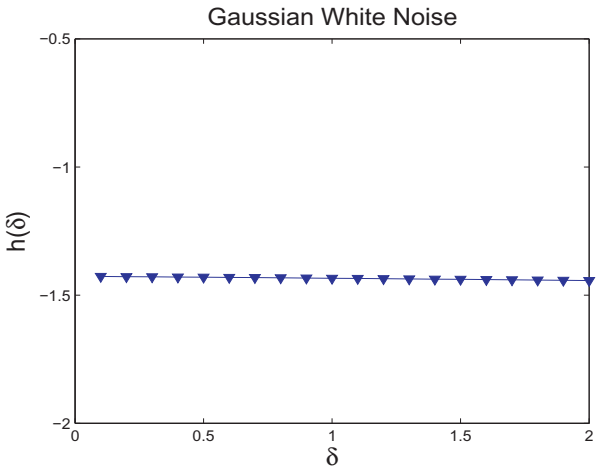

Fig. 7. The corresponding slopes $h(\delta)$ versus δ for Gaussian White Noise with results obtained from the best fitting straight line of $\ln S_{q,\delta}$ versus $\ln q$ for each δ.

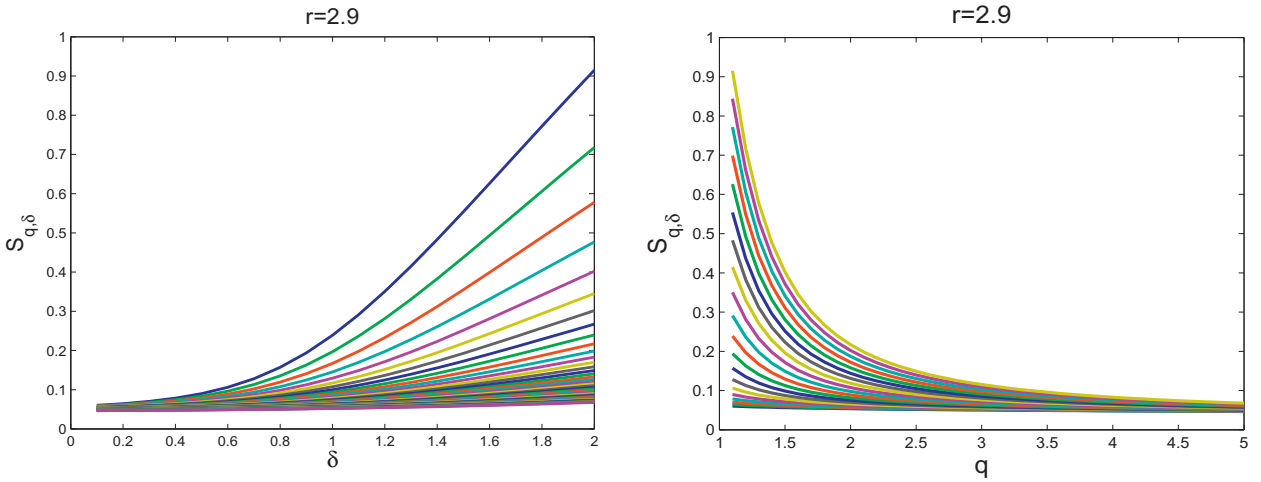

Fig. 8. Values of two-index entropy $S_{q,\delta}$ versus q and δ separately for Logistic map when $r = 2.9$. In the first graph, the upper curve presents smaller parameter q, and in the second graph, the upper curve presents bigger parameter δ.

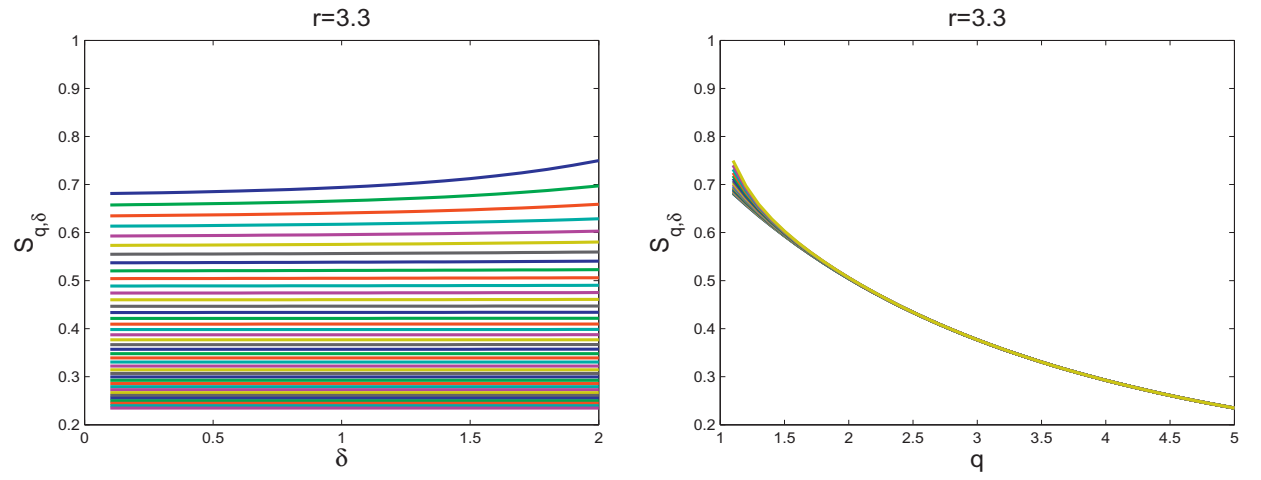

Fig. 9. Values of two-index entropy $S_{q,\delta}$ versus q and δ separately for Logistic map when $r = 3.3$. In the first graph, the upper curve presents smaller parameter q, and in the second graph, the upper curve presents bigger parameter δ.

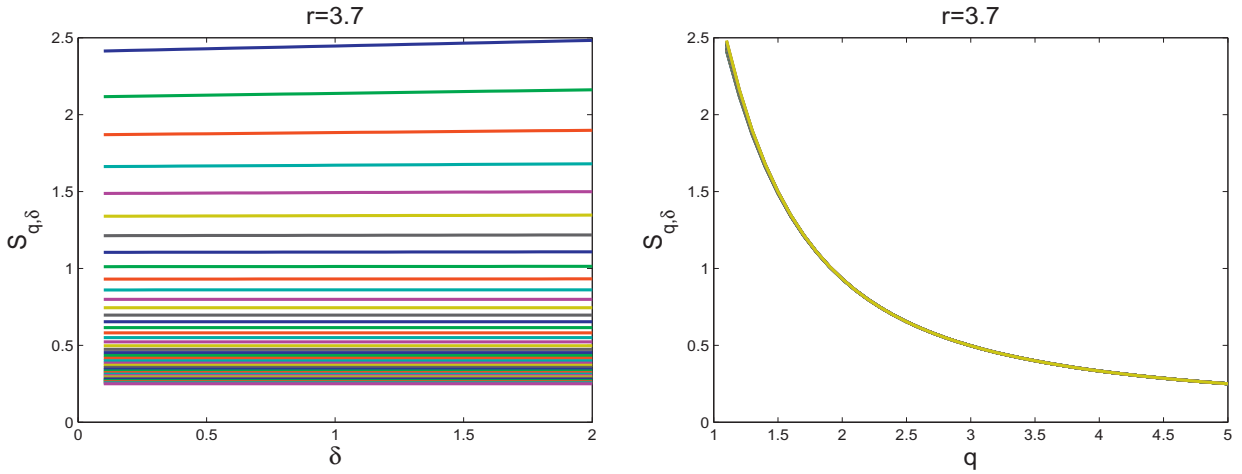

Fig. 10. Values of two-index entropy $S_{q,\delta}$ versus q and δ separately for Logistic map when $r = 3.7$. In the first graph, the upper curve presents smaller parameter q, and in the second graph, the upper curve presents bigger parameter δ.

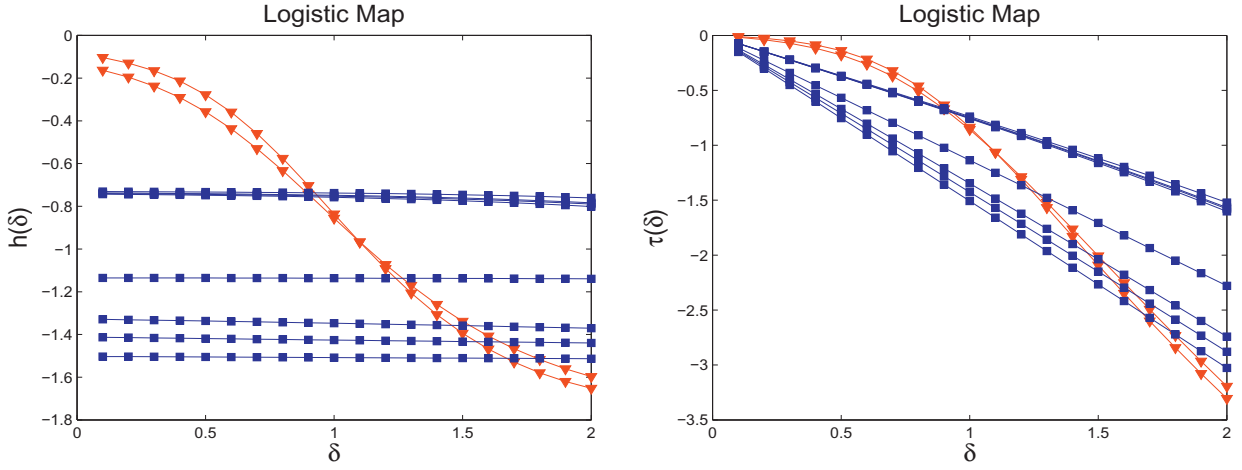

Fig. 11. The corresponding slopes $h(\delta)$ and $\tau(\delta)$ versus δ for logistic map with results obtained from the best fitting straight line of $\ln S_{q,\delta}$ versus $\ln q$ for each δ, where we set parameter r range from 2.8 to 3.7 and the step size is 0.1. (For interpretation of the references to color in this figure, the reader is referred to the web version of this article.)

Finally, in this case ($r = 3.7$, Fig. 10), the periodic bifurcation is abrupt and chaos takes the place of periodicity. The probabilities turn to be approximately equal. Using Eq. (14), we can draw the conclusion that parameter δ has nothing to do with entropy $S_{q,\delta}$ approximately. We can see this case is similar with the case for Gaussian White Noise. The two-index entropy for $(q, \delta) = (1.1, 1)$ is about 2.48.

With the increasing of r, the sequence turns to be more out-of-order and the probabilities approximate being equal. On the one hand, the entropy measures for $(q, \delta) = (1.1, 1)$ trend to be bigger and bigger and it shows the complexity grows. On the other hand, the parameter δ has less influence, which can be indicated by the parallelism degree of curves for $S_{q,\delta}$ versus δ and aggregation degree of curves for $S_{q,\delta}$ versus q, on the entropy $S_{q,\delta}$. Therefore, using the two-index entropy, we can estimate the complexity of series by the value of two-index entropy directly or analyzing the influence that parameter δ has on the entropy $S_{q,\delta}$. In order to analyze the influence, we will take the scaling exponent $h(\delta)$ as an efficient method. Even if the randomness for different sequences are proximate or equal, the scaling exponent can also distinguish the systems which generating the sequences. The scaling exponents $h(\delta)$ are determined from the slopes of the different lines ($\ln S_{q,\delta}$ versus $\ln q$).

For the first graph in Fig. 11, we will search in two sides. On the one hand, for $r \geq 3.0$, the scaling exponent can be seen as a constant versus parameter δ shown as the blue curves in Fig. 11, thus the series in these cases is out of order. For $r < 3.0$, the stability of the series contributes to the multi-scaling of the two-index entropy shown as the red curves in Fig. 11. On the other hand, when the series is instability, despite all the slopes curves for $h(\delta)$ versus δ are approximately equal to zero, the constants which the scaling exponents for different parameter r approach to differ from each other. When $3.0 \leq$

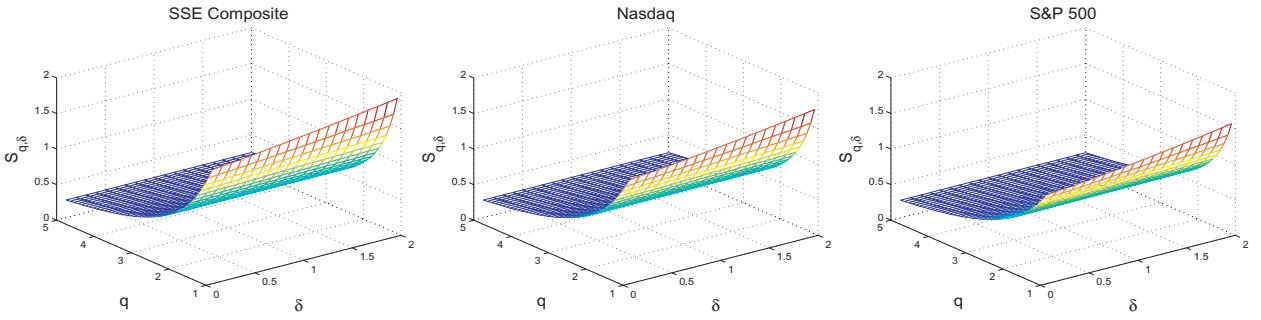

Fig. 12. The three-dimensional relationships between $S_{q,\delta}$, q and δ for S&P 500, Nasdaq and SSE Composite.

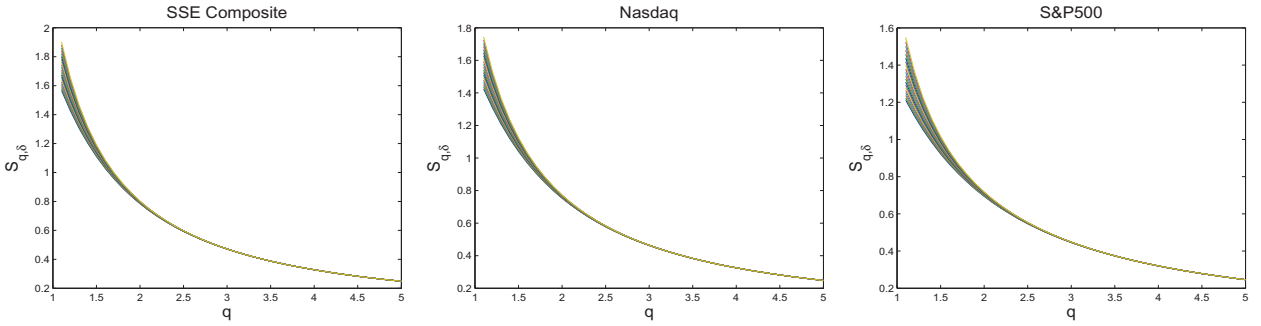

Fig. 13. Values of two-index entropy $S_{q,\delta}$ versus q for the cases S&P 500, Nasdaq and SSE Composite. Curves of different colors represent different parameters δ.

$r \leq 3.3$, the constants are similar shown as the upper four blue curves. That is because the sequences approaches to two different values for the range of r. Then with the increasing of r, the periodic bifurcation becomes more and more, so there are significant differences in the scaling exponents $h(\delta)$ shown as the lower four blue curves. That is the principle which we base on to analyze the influence of parameter δ on entropy $S_{q,\delta}$.

In the second graph in Fig. 11, for $r \geq 3$, the slope of exponent $\tau(\delta)$ versus δ can be seen as a constant versus parameter δ shown as the blue curves in Fig. 11. For $r \leq 3.0$, the stability of the series contributes to the multifractal of the two-index entropy shown as the red curves in Fig. 11. As a transformation of $h(\delta)$, $\tau(\delta)$ is also an efficient way to estimate the influence which we have mentioned above.

5. Classifying the financial markets based on refined two-index entropy

The new two-index entropy is appropriate for measuring the entropy of more complex systems. The multi-scaling analysis about the two-index entropy can show the different properties of entropy for different scales. The multi-scaling analysis can also be used to distinguish various dynamic systems. To investigate the utility of the two-index entropy of quantifying the complexity and detecting the systems generating the series, an experiment based on real series has been carried out with details as follows.

Considering the complexity and similarity of series, in this study, the application experiment is to verify the applicability of two-index entropy in financial series. The two-index entropy method will be applied to analyze the logarithmic return series of several markets, like S&P 500, Nasdaq and SSE Composite, under consideration $x(n) = \ln(S(n)) - \ln(S(n-1))$, where $S(n)$ denotes the close price at time n. The data was collected from the Yahoo Financial web site. The length of series is $N = 6140$ and we set the date range from Dec 19th, 1990 to Dec 5th, 2014.

Using Eq. (13), we obtain the values of two-index entropy for the three markets. Actually, analysis on the logarithmic return series by the two-index entropy can be seen as the method of entropy measure considering both the happening frequency of fluctuations and the range of fluctuations. By controlling variables, we can take concrete analysis on two-index entropy.

Fig. 12 shows the three-dimensional images about the entropy of the three markets (S&P 500, Nasdaq and SSE Composite) and Fig. 13 shows them from another perspective. The graphs for the three financial markets are similar both in Figs. 12 and 13. Entropy measure of each time series decreases with the increasing value of parameter q. From Fig. 13, the dispersions of curves for the three images are small, so the impact which parameter δ has on two-index entropy is small. And then, the complexities of them are approximative but outstanding. In Fig. 13, We can find that the entropy measure is about 1.7121 which occurs at point $(q, \delta) = (1.1, 1)$ for the series of SSE Composite. And the entropy measure is about 1.3457 for S&P 500

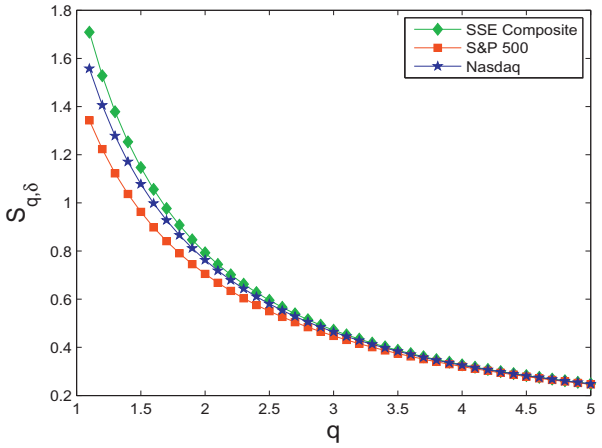

Fig. 14. The curves ($S_{q,\delta}$ versus q) for S&P 500, Nasdaq and SSE Composite when $\delta = 1$.

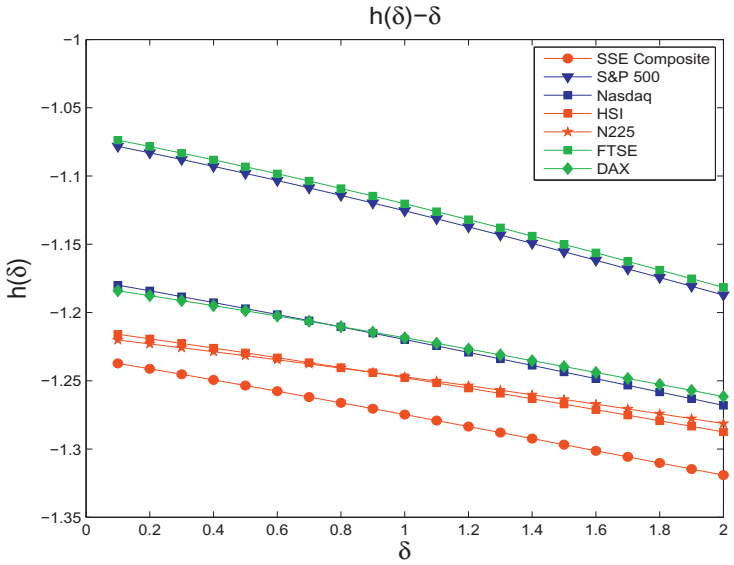

Fig. 15. Values of the scaling exponent $h(\delta)$ for return series of seven financial markets: SE Composite, S&P 500, Nasdaq, HSI, N225, FTSE and DAX.

and 1.5652 for Nasdaq. This indicates the return series of SSE Composite is more complex than S&P 500 and Nasdaq. Fig. 14 shows the curves ($S_{q,\delta}$ versus q) for the three financial markets when $\delta = 1$. And then the complexity of the three financial markets can be compared roughly by Fig. 14. What we need stress is that this method is suitable for the series which comes from similar dynamic system. That is because when the randomness is strong, according to Eq. (20), the value of two-index entropy only relates to data size W and element size N. Because the values of entropy measure are approximative and the trends of entropy versus parameters are similar (shown as Figs. 12 and 13), in what follows, we will pay attention to the scaling exponent $h(\delta)$ and compare it to the simulation achievements.

In order to strengthen the contrast, we add the number of time series to 7 and these financial markets are SSE Composite, S&P 500, Nasdaq, HSI, N225, FTSE and DAX. Then, we calculated the values of scaling exponents $h(\delta)$ for return series of every stock markets. As shown in Fig. 15, the Asian financial time series like SSE Composite, HSI and N225 have smaller scaling exponent $h(\delta)$. That means the series from Asian financial market shows more complicated and instable than European and American. What is more, the scaling exponent $h(\delta)$ for SSE Composite is particular. But the scaling exponents for S&P 500 and FTSE, NASDAQ and DAX, HIS and N225 are similar in pairs and it indicates the dynamic systems they come from are analogous. So far we have classified these complex return series of financial markets roughly by analyzing the scaling exponent of two-index entropy.

Now the simulation results are used to analyze the difference between these financial markets. We choose the values of scaling exponents $h(1)$ as a parameter which will be compared with simulation data and then group the complex dynamic systems. Here are some test results obtained from binomial multifractal series experiments ($h(1)$ versus a) Table 1 and

Table 1
$h(1)$ and parameter a obtained numerically from binomial multifractal series experiments.

a	0.65	0.62	0.61	0.6	0.59	0.58
$h(1)$	−0.9675	−1.1267	−1.1501	−1.2537	−1.2793	−1.2842

Table 2
$h(1)$ and parameter r obtained numerically from Logistic Map experiments ($x_0 = 0.6$).

r	3.5	3.55	3.56	3.562	3.6
$h(1)$	−1.126	−1.2134	−1.2505	−1.2760	−1.4226

Table 3
The $h(1)$ for the seven financial markets and simulation parameters a or r corresponding these $h(1)$ according to Tables 1 and 2.

Financial market	$h(1)$	a from binomial multifractal series	r from logistic map
SSE composite	−1.2748	0.59	3.562
S&P 500	−1.1255	0.62	3.500
Nasdaq	−1.2198	0.60–0.61	3.550
HSI	−1.2477	0.60	3.560
N225	−1.2471	0.60	3.560
FTSE	−1.1203	0.62	3.500
DAX	−1.2185	0.60–0.61	3.550

Logistic Map experiments ($h(1)$ versus r) Table 2. The $h(1)$ for the seven financial markets are shown in the second column in Table 3.

Table. 3 shows that $h(1)$ for SSE Composite is −1.2748 and then SSE Composite can been identified as the dynamic system which is similar to the binomial multifractal series when $a = 0.59$ or Logistic Map when $x_0 = 0.6$ and $r = 3.562$. Other similar corresponding relations are shown in the third and fourth column in Table 3. Using the corresponding –relationship with parameter a of simulation experiments, these seven financial markets can be divided into 4 groups. Group1 consists of S&P 500 and FTSE; Group2 consists of Nasdaq and DAX; Group3 consists of HSI and N225, and Group4 consists of SSE Composite. We can see the different simulation experiments lead to the same classification.

All in all, all the 7 markets shows analogous complexity considering the randomness. Also, the series from Asian financial market shows more complicated and instable than European and American. Some financial markets from different regions show some statistical similarity which we can take advantage of to classify them.

6. Conclusion

This work proposes a refined two-index entropy $S_{q,\delta}$ which can be seen as a generalization of the well-known nonextensive entropy S_q. According to what we have mentioned in Sections 3.1 and 3.2, apart from widening the range of applicability of statistical mechanical concepts to many complex systems, the refined two-index entropy can be carried on multi-scale analysis more effectively and conveniently. Using the two-index entropy, we can estimate the complexity of series by the value of two-index entropy directly or the influence that parameter δ has on the entropy $S_{q,\delta}$. In order to analyze the influence, we take the scaling exponent $h(\delta)$ as an efficient method. Specifically, for more complex system, the value of two-index entropy is smaller and the correlation between parameter δ and entropy $S_{q,\delta}$ is weaker. At the same time, the scaling exponent $h(\delta)$ is smaller and more stable.

Compared to other families of entropies, this refined two-index entropy can measure the complexity from more comprehensive perspectives. Therefore, it has extensive applications in studying some troublesomely complex systems and classifying the similar complex systems. We also present several simulation series to evaluate the effectiveness of the two-index entropy. For the series with various complexities, the refined two-index entropy $S_{q,\delta}$ and the scaling exponent $h(\delta)$ perform actively. Combined with the achievement of simulation series, the scaling exponent $h(\delta)$ is utilized to classify several financial markets from different regions of the world effectively.

Acknowledgment

The financial supports from the funds of the China National Science (61371130) and the Beijing National Science (4122059) are gratefully acknowledged.

References

[1] Penrose O. Foundations of statistical mechanics: A deductive treatment. New York: Dover Publications; 2005.

[2] Tsallis C. Thermostatistically approaching living systems: Boltzmann–Gibbs or nonextensive statistical mechanics. Commun Nonlinear Sci Numer Simul 2006;3:1–22.
[3] Gallavotti G. Statistical mechanics: A short treatise. Berlin: Springer; 1999.
[4] Adam C, Piotr J. Set of possible values of maximal Lyapunov exponents of discrete time-varying linear system. Commun Nonlinear Sci Numer Simul 2008;44:580–3.
[5] Hernan DS, German P. Scaling of entropy and multi-scaling of the time generalized image-entropy in rainfall and streamflows. Commun Nonlinear Sci Numer Simul 2015;423:11–26.
[6] Marco M. On the q-parameter spectrum of generalized information-entropy measures with no cut-off prescriptions. Commun Nonlinear Sci Numer Simul 2006;357:288–94.
[7] Tsallis C. Possible generalization of Boltzmann–Gibbs statistics. J Stat Phys 1988;52:479–87.
[8] Cressie N, Read T. Multinomial goodness of fit tests. J R Stat Soc Ser B 1984;46:440–64.
[9] Read T, Cressie N. Goodness of fit statistics for discrete multivariate data. New York: Springer; 1988.
[10] Hajmohammadi MR, Maleki H, Lorenzini G, Nourazar SS. Effects of CU and AG nano-particles on flow and heat transfer from permeable surfaces. Adv Powder Technol 2015;26:193–9.
[11] Hajmohammadi MR, Lorenzini G, Joneydi Shariatzadeh O, Biserni C. Evolution in the design of v-shaped highly conductive pathways embedded in a heat generating piece. J Heat Transf 2015;137(6):061001.
[12] Ko TH, Ting K. Optimal Reynolds number for the fully developed laminar forced convection in a helical coiled tube. Energy 2006;31:2142–52.
[13] Hajmohammadi MR, Nourazar SS, Campo A, Poozesh S. Optimal discrete distribution of heat flux elements for in-tube laminar forced convection. Int J Heat Fluid Flow 2013;40:89–96.
[14] Pouzesh A, Hajmohammadi MR, Poozesh S. Investigations on the internal shape of constructal cavities intruding a heat generating body. Therm Sci 2015;19:609–18.
[15] Hajmohammadi MR, Poozesh S, Rahmani M, Campo A. Heat transfer improvement due to the imposition of non-uniform wall heating for in-tube laminar forced convection. Appl Therm Eng 2013;61:268–77.
[16] Hajmohammadi MR, Shirani E, Salimpour MR, Campo A. Constructal placement of unequal heat sources on a plate cooled by laminar forced convection. Int J Therm Sci 2012;60:13–22.
[17] Hajmohammadi MR, Poozesh S, Nourazar SS, Manesh AH. Optimal architecture of heat generating pieces in a fin. J Mech Sci Technol 2013;27(4):1143–9.
[18] Hajmohammadi MR, Poozesh S, Hosseini R. Radiation effect on constructal design analysis of a t-y-shaped assembly of fins. J Therm Sci Technol 2012;7:677–92.
[19] Hajmohammadi MR, Campo A, Nourazar SS, Ostad AM. Improvement of forced convection cooling due to the attachment of heat sources to a conducting thick plate. J Heat Transf 2013;135:124504-1.
[20] Hajmohammadi MR, Joneydi Shariatzadeh O, Moulod M, Nourazar SS. PHI and PSI shaped conductive routes for improved cooling in a heat generating piece. Int J Therm Sci 2014;77:66–74.
[21] Hajmohammadi MR, Moulod M, Joneydi O, Campo A. Effect of a thick plate on the excess temperature of ISO-heat flux heat sources cooled by laminar forced convection flow: Conjugate analysis. Numer Heat Transf 2014;66:205–16.
[22] Najafi H, Najafi B, Hoseinpoori P. Energy and cost optimization of a plate and fin heat exchanger using genetic algorithm. Appl Therm Eng 2011;31:1839–47.
[23] Tsallis C. Is the entropy SQ extensive or nonextensive? Astrophys Space Sci 2006;305:261–71.
[24] Touchette H. When is a quantity additive, and when is it extensive? Physica A 2002;305:84–8.
[25] Hanel R, Thurner S. When do generalized entropies apply? How phase space volume determines entropy. Eur Phys Lett 2011;96:50003.
[26] Borges EP, Tsallis C, Miranda GEV, Andrade RFS. Mother wavelet functions generalized through q-exponentials. J Phys A 2004;37:9125–38.
[27] Tsallis C, Gell-mann M, Sato Y. Asymptotically scale-invariant occupancy of phase space makes the entropy s_q extensive. Proc Natl Acad Sci 2005;102(43):15377–82.
[28] Tamas SB, Viktor GC. A q-parameter bound for particle spectra based on black hole thermodynamics with Renyi entropy. Commun Nonlinear Sci Numer Simul 2013;726:861–5.
[29] Tsallis C, Cirto LJL. Black hole thermodynamical entropy. Eur Phys J C 2013;73:2487.
[30] Komatsu N, Kimura S. Entropic cosmology for a generalized black-hole entropy. Phys Rev D 2013;88:083534.
[31] Ribeiro MS, Tsallis C, Nobre FD. Probability distributions extremizing the nonadditive entropy s_δ and stationary states of the corresponding nonlinear Fokker–Planck equation. Phys Rev E 2013;88:052107.
[32] Abe S. A note on the q-deformation-theoretic aspect of the generalized entropies in nonextensive. Phys Lett A 1997;224:326–30.
[33] Landsberg PT, Vedral V. Distributions and channel capacities in generalized statistical mechanics. Phys Lett A 1998;247:211–17.
[34] Kaniadakis G. Non-linear kinetics underlying generalized statistics. Phys A 2001;296:405–25.
[35] Kaniadakis G. Statistical mechanics in the context of special relativity. Phys Rev E 2002;66:056125.
[36] Kaniadakis G, Lissia M, Scarfone AM. Two-parameter deformations of logarithm, exponential and entropy: A consistent framework for generalized statistical mechanics. Phys Rev E 2005;71:046128.
[37] Chandrashekar R, Segar J. Adiabatic thermostatistics of the two parameter entropy and the role of Lambert's image-function in its applications. Commun Nonlinear Sci Numer Simul 2013;392:4299–315.
[38] Sharma BD, Taneja IJ. Entropy of type (α, β) and other generalized measure in information theory. Metrika 1975;22:205–15.
[39] Borges EP, Roditi I. A family of nonextensive entropies. Phys Lett A 1998;246:399–402.
[40] Tempesta P. Group entropies, correlation laws, and zeta functions. Phys Rev E 2011;84:021121.
[41] Somayeh A. A set of new three-parameter entropies in terms of a generalized incomplete gamma function. Commun Nonlinear Sci Numer Simul 2013;392:1972–6.
[42] Renyi A. On measures of entropy and information. Proceedings of the Fourth Berkeley Symposium on Mathematical Statistics and Probability, vol 1; 1961. p. 547–61.
[43] Morimoto T. Markov processes and the h-theorem. J Phys Soc Jap 1963;12:328–31.
[44] Gorban AN. Maxallent: Maximizers of all entropies and uncertainty of uncertainty. Comput Math Appl 2013;65(10):1438–56.
[45] Callen HB. Thermodynamics and an Introduction to Thermostatistics. New York: Wiley; 1985.
[46] Kantelhardt JW, Zschiegner SA, K-Bunde E, Havlin S, Bunde A, Stanley HE. Multifractal detrended fluctuation analysis of nonstationary time series. Physica A 2002;316:87–114.
[47] Hajmohammadi MR, Moulod M, Joneydi Shariatzadeh O, Nourazar SS. Essential reformulations for optimization of highly conductive inserts embedded into a rectangular chip exposed to a uniform heat flux. J Mech Eng Sci 2014c;228(13):2337–46.
[48] Hajmohammadi MR, Pouzesh A, Poozesh S. Controlling the heat flux distribution by changing the thickness of heated wall. J Basic Appl Sci Res 2012c;2(7):7270–5.
[49] Hajmohammadi MR, Moulod M, Joneydi Shariatzadeh O, Nourazar SS. New methods to cope with temperature elevations in heated segments of flat plates cooled by boundary layer flow. Therm Sci 2013e;00:159.
[50] Hajmohammadi MR, Salimpour MR, Saber M, Campo A. Detailed analysis for the cooling performance enhancement of a heat source under a thick plate. Energy Convers Manag 2013f;76:691–700.
[51] Wong CY, Wilk G. Tsallis fits to p_t spectra and multiple hard scattering in pp collisions at the LHC. Phys Rev D 2013;87:114007.
[52] Tamarit FA, Cannas SA, Tsallis C. Sensitivity to initial conditions in the Bak–Sneppen model of biological evolution. Eur Phys J B 1998;1:545–8.
[53] Umarov S, Tsallis C, Steinberg S. On a q-central limit theorem consistent with nonextensive statistical mechanics. Milan J Math 2008;76:307–28.

[54] Umarov S, Tsallis C, Gell-Mann M, Steinberg S. Generalization of symmetric α-stable levy distributions for $q > 1$. J Math Phys 2010;51:033502.
[55] Tsallis C, Gell-Mann M, Sato Y. Asymptotically scale-invariant occupancy of phase space makes the entropy s_q extensive. Natl Acad Sci USA 2005b;102:15377–82.
[56] Caruso F, Tsallis C. Nonadditive entropy reconciles the area law in quantum systems with classical thermodynamics. Phys Rev E 2008;78:021102.
[57] Saguia A, Sarandy MS. Nonadditive entropy for random quantum spin-s chains. Phys Lett A 2010;374:3384–8.
[58] Barabasi AL, Vicsek T. Multifractality of self-affine fractals. Phys Rev A 1991;44:2730–3.
[59] Cysarz D, Porta A, Montano N, Leeuwen PV, Kurths J, Wessel N. Quantifying heart rate dynamics using different approaches of symbolic dynamics. Eur Phys J Spec 2013;222:487–500.
[60] Silva LEV, Murta JL. Evaluation of physiologic complexity in time series using generalized sample entropy and surrogate data analysis. Chaos 2012;22:043105.
[61] Bandt C, Pompe B. Permutation entropy – A natural complexity measure for time series. Phys Rev Lett 2002;88(17):174102.
[62] Feder J. Fractals. New York: Plenum Press; 1988.
[63] Peitgen HO, Urgens HJ, Saupe D. Chaos and fractals. New York: Springer; 1992.